Available online at www.sciencedirect.com
SCIENCE DIRECT®
Surface Science 547 (2003) 19–26
SURFACE SCIENCE
www.elsevier.com/locate/susc

X-ray standing wave study of the Sr/Si(0 0 1)-(2 × 3) surface

D.M. Goodner [a], D.L. Marasco [b], A.A. Escuadro [a], L. Cao [a], B.P. Tinkham [a], M.J. Bedzyk [a,c,*]

[a] *Materials Science Department and Materials Research Science and Engineering Center, Northwestern University, 2220 N. Campus Drive, Evanston, IL 60208, USA*
[b] *Department of Physics and Astronomy, Northwestern University, Evanston, IL 60208, USA*
[c] *Argonne National Laboratory, Argonne, IL 60439, USA*

Received 5 August 2003; accepted for publication 22 September 2003

Abstract

Sub-monolayer surface phases of Sr on Si(0 0 1) have been studied with low-energy electron diffraction (LEED) and X-ray standing waves (XSW). A (3×1) phase was observed after depositing 0.6–0.8 ML Sr on room-temperature Si(0 0 1). Annealing at 750–800 °C caused a portion of the Sr to desorb and resulted in a sharp (2×3) LEED pattern. Normal Si(0 0 4) and off-normal Si(0 2 2) and Si(1 1 1) XSW measurements made on the (2×3) phase indicate that Sr atoms must sit at either cave or bridge sites. The XSW results also suggest that if a sufficiently low anneal temperature is used, the (2×3) phase co-exists with short-range ordered regions of Sr atoms located at valley-bridge sites.

Keywords: Surface structure, morphology, roughness, and topography; Low index single crystal surfaces; Alkaline earth metals; Silicon; Molecular beam epitaxy; X-ray standing waves; Low energy electron diffraction (LEED)

1. Introduction

Sub-monolayer coverages of Sr on Si(0 0 1) surfaces are known to form ordered two-dimensional phases. Interest in Sr/Si(0 0 1) surfaces is primarily driven by efforts to integrate various Sr-containing oxides onto Si-based microelectronics devices. Early Sr/Si(0 0 1) studies [1–3] were largely motivated by interest in growing films of high-T_C superconducting Bi–Sr–Cu–O on Si [4,5]. More recently, $SrTiO_3$ has been viewed as a likely candidate to replace SiO_2 as the gate dielectric in field effect transistors [6] due to the high dielectric constant of $SrTiO_3$ relative to SiO_2 and the small lattice mismatch between the $SrTiO_3$(1 0 0) and Si(1 1 0) planes. Bulk thermodynamic arguments [7,8] as well as cross-sectional transmission electron microscopy studies of $SrTiO_3$ films on Si(0 0 1) [9,10] indicate that the formation of unwanted Si-oxides at the $SrTiO_3$–Si interface can be minimized or prevented altogether by preceding $SrTiO_3$ growth with the formation of an ordered, two-dimensional phase consisting of sub-monolayer amounts of Sr on the Si(0 0 1) surface.

Low-energy electron diffraction (LEED) and Auger electron spectroscopy (AES) studies [3,11] have revealed the existence of several coverage and

* Corresponding author. Tel.: +1-847-491-3570; fax: +1-847-467-2269.
E-mail address: bedzyk@northwestern.edu (M.J. Bedzyk).

0039-6028/$ - see front matter © 2003 Elsevier B.V. All rights reserved.
doi:10.1016/j.susc.2003.09.031

temperature dependent Sr/Si(0 0 1) surface reconstructions, including (2×3), (2×1), (3×1) and (5×1) phases for Sr coverage, $\Theta < 1.5$ ML. The (2×3) phase has been reported to form at temperatures between 700 and 850 °C and Sr coverages ranging from 1/6 to 1/3 ML. Based on scanning tunneling microscopy (STM) results, Bakhtizin et al. [12,13] proposed that the (2×3) phase saturates at a coverage of 1/3 ML with Sr atoms occupying 2/3 of the cave sites on a dimerized Si(0 0 1) surface, and X-ray photoemission spectroscopy (XPS) measurements in conjunction with Rutherford backscattering spectrometry (RBS) [14] showed a (2×3) surface to contain 0.35 ML Sr. Hu et al. [11] however, used LEED, AES and STM observations to argue that the (2×3) phase actually saturates at 1/6 ML with one Sr atom per surface unit cell, but did not present any atomic-scale structural model. Variations in the intensities of reflection high-energy electron diffraction spots monitored during Sr deposition onto heated (~700 °C) Si(0 0 1) also suggest that the (2×3) phase saturates at 1/6 ML [9,15].

We have used in situ LEED, AES and X-ray standing wave (XSW) measurements to study submonolayer amounts of Sr on Si(0 0 1) and present an atomic-scale structural model of the (2×3) phase formed by annealing at 750–800 °C. Our XSW results also indicate that near the low end of this temperature regime, the (2×3) phase co-exists with a secondary phase that exhibits primarily short-range order.

2. Experiment

Experiments were conducted at the 12ID-D X-ray undulator BESSRC-CAT experimental station at the Advanced Photon Source, Argonne National Laboratory. Molecular beam epitaxy sample preparation, AES, LEED and XSW measurements were performed in an ultra-high vacuum (UHV) system with a base pressure $\sim 1.5\times10^{-10}$ Torr.

Single-crystal Si(0 0 1) samples were treated with a modified Shiraki etch [16] and mounted in a strain-free manner onto molybdenum sample-holders prior to introduction into the UHV system. After degassing ~12 h at 400–600 °C, samples were annealed for 15 min at 850–900 °C to remove the chemically grown SiO_2 film and produce a sharp, two-domain (2×1) LEED pattern indicating a dimerized Si(0 0 1) surface. AES showed C and O contamination levels to be less than 0.02 ML ($1\ \text{ML} = 6.78\times10^{14}$ atoms/cm^2).

An effusion cell was used to deposit 0.6–0.8 ML Sr at a rate of 0.06 ML/min onto the room-temperature (RT) Si(0 0 1) substrates, resulting in a (3×1) LEED pattern. Subsequent anneals at 750 and 800 °C caused portions of the Sr to desorb and resulted in sharp (2×3) LEED patterns. The Sr coverage was determined in UHV by comparing the intensity of the Sr Kα fluorescence from the samples to that of a Sr-implanted Si(0 0 1) standard calibrated by RBS. Sample temperature was monitored using an optical pyrometer and a thermocouple mounted on the sample stage.

Using an incident photon energy of 18.5 keV, UHV XSW measurements were conducted after each post-deposition anneal by scanning the sample in angle through the Si (0 0 4), (0 2 2) and (1 1 1) Bragg conditions. The incident beam from the undulator was filtered by a high-heat-load Si(1 1 1) monochromator followed by a post-monochromator consisting of a pair of detuned nondispersive Si channel-cut crystals. The d-spacing of the post-monochromator matched that of the sample. For more XSW experimental details, see Refs. [17,18]. During each scan, the diffracted beam intensity was monitored with a photodiode, and the X-ray fluorescence spectra were collected by a Si (Li) solid state detector. The Sr coherent fractions (f_H) and coherent positions (P_H) were determined by fitting the reflectivity and normalized Sr Kα fluorescence yield data to dynamical diffraction theory. Following the formalism of Ref. [18], f_H can be defined as:

$$f_H = Ca_H D_H \tag{1}$$

C is the ordered fraction of Sr atoms, and D_H is the Debye–Waller factor. The geometrical factor a_H is the modulus of the normalized geometrical structure factor and is given by:

$$a_H = \frac{1}{C}\left|\sum_{j=1}^{N}\left[c_j \exp\left(2\pi i \boldsymbol{H}\cdot\boldsymbol{r}_j\right)\right]\right| \tag{2}$$

where c_j and $\boldsymbol{r}_j$ are the respective occupancy (as a fraction of C) and position vector (within the bulk Si unit cell) of the jth site onto which Sr atoms preferentially adsorb. P_H is the phase of the normalized geometrical structure factor and can be written as:

$$P_H = \frac{1}{2\pi} \arg\left[\sum_{j=1}^{N} \left[c_j \exp\left(2\pi i \boldsymbol{H}\cdot\boldsymbol{r}_j\right)\right]\right] \quad (3)$$

3. Results/discussion

3.1. LEED and Sr coverage measurements

All previously reported sub-monolayer Sr/Si(0 0 1) surface phases exhibiting long-range order have been prepared by annealing the surface during (or after) at least part of the deposition process. There has been one report of a 7/8 ML (3×1) phase formed by depositing the final 3/8 ML onto RT Si(0 0 1), but this process was preceded by the deposition of 1/2 ML Sr onto 700 °C Si to form a well-ordered (2×1) phase [15]. Fig. 1(a) shows an example of the (3×1) LEED patterns we have observed on surfaces prepared by depositing 0.6–0.8 ML Sr onto a Si(0 0 1)-(2×1) surface held at RT during the entire deposition process.

Annealing the as-deposited (3×1) phase for 10 min at 750 °C caused the Sr coverage to decrease to 0.19 ± 0.04 ML and resulted in the (2×3) LEED pattern shown in Fig. 1(c). This temperature is approximately 50 °C lower than that previously cited [3,11] as the minimum value required to form the (2×3) phase after Sr deposition onto RT Si(0 0 1). We have in fact observed a (2×3) surface after annealing the as-deposited surface at just 720 °C, although the LEED pattern, shown in Fig. 1(b), was accompanied by 4× streaks. This temperature discrepancy may be due to the fact that there is some time-dependence involved in the desorption process. When the duration of a 750 °C anneal was limited to just 1 min, we observed the higher coverage (2×1) phase [3,11,14,15,19]. Our XSW analysis of the (2×1) phase will be reported elsewhere. After the surface was heated to 800 °C for 1 min, the (2×3) periodicity remained, but the

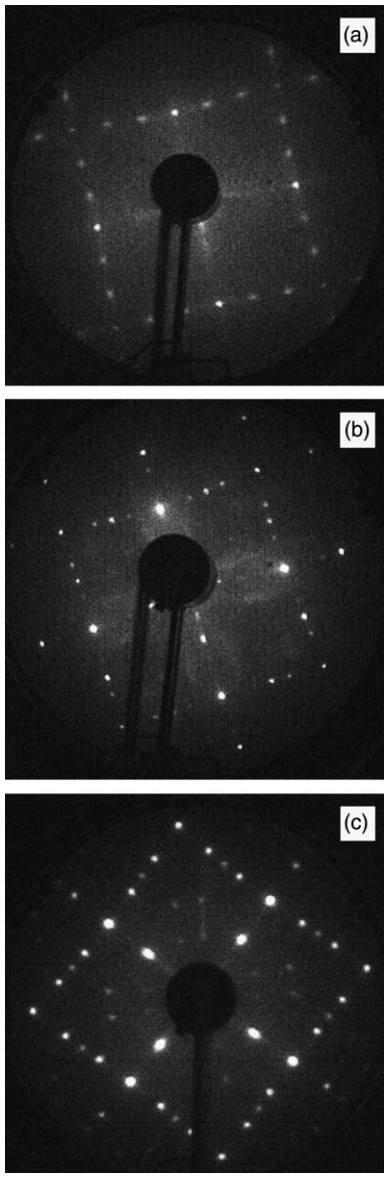

Fig. 1. (a) (3×1) LEED pattern observed after depositing 0.78 ML Sr onto RT Si(0 0 1)-(2×1). (b) (2×3) pattern with 4× streaks obtained after annealing surface in (a) for 10 min at 720 °C. (c) Pure (2×3) pattern resulting from 10 min anneal at 750 °C.

Sr coverage decreased to 0.12 ± 0.03 ML. For simplicity, the (2×3) surfaces resulting from the 10 min 750 °C and 1 min 800 °C anneals shall be referred to as the "750 °C surface" and "800 °C surface", respectively. The Sr coverage and LEED

Table 1
Summary of the Sr coverage and LEED patterns observed immediately after RT deposition and after annealing at 750 and 800 °C

Anneal temperature (°C)	Coverage (ML)	LEED pattern	P_{004}	f_{004}	P_{022}	f_{022}	P_{111}	f_{111}
800	0.12(3)	(2×3)	0.86(1)	0.56(2)	0.42(1)	0.59(4)	0.63(1)	0.41(2)
750	0.19(4)	(2×3)	0.92(1)	0.24(2)	0.52(1)	0.40(2)	–	–
RT	0.6–0.8	(3×1)	–	–	–	–	–	–

The coverage range cited for the RT (3×1) phase spans the range of coverages observed on multiple RT prepared (3×1) samples. Model-independent XSW measured P_H and f_H values determined for surfaces annealed at 750 and 800 °C are also listed.

periodicity of these two surfaces and the as-deposited (3×1) surfaces are summarized in Table 1.

3.2. XSW analysis of the 800 °C surface

Experimental data and the corresponding theoretical fits from normal Si(0 0 4) and off-normal Si(0 2 2) XSW measurements of the 800 °C surface are shown in Fig. 2. The f_H and P_H values determined from each of these measurements, along with the results of a Si(1 1 1) XSW measurement, are summarized in Table 1. Assuming Sr occupies only one type of site, the coherent position $P_{004} = 0.86$ corresponds to the ordered Sr atoms sitting 1.17 Å above the bulk plane of second layer Si atoms. If these adatoms are assumed to occupy a high symmetry site, their 3-D position relative to the underlying Si lattice can be determined by considering the P_{004} value in conjunction with just one additional XSW measurement using an off-normal set of Bragg diffraction planes. The high symmetry sites on the dimerized and undimerized Si(0 0 1) surface are shown in Fig. 3. The measured P_{022} and P_{004} values are in close agreement with the relationship:

$$P_{022} = \frac{P_{004}}{2} \tag{4}$$

a geometrical symmetry requirement for the occupation of cave or bridge sites on a dimerized Si(0 0 1) surface. This relationship would also be expected if Sr atoms were to occupy bridge sites on an undimerized Si(0 0 1) surface. Note that XSW measurements project the distribution of atomic positions into the 3-D primitive unit cell of the underlying bulk crystal. The cave and bridge sites on the dimerized surface both represent positions equivalent to that of the bridge site on an undimerized surface within this bulk primitive unit cell.

If two adatoms on the Si(0 0 1) surface occupy identical sites but are located on adjacent terraces separated by a monoatomic step, these adatoms occupy equivalent positions relative to the bulk Si(0 0 4) and Si(0 2 2) Bragg diffraction planes but are in nonequivalent positions relative to the bulk Si(1 1 1) Bragg diffraction planes. The geometrical symmetry relationships between P_{111} and P_{004} for adatoms occupying cave or bridge sites on a two-domain (2×3) surface are:

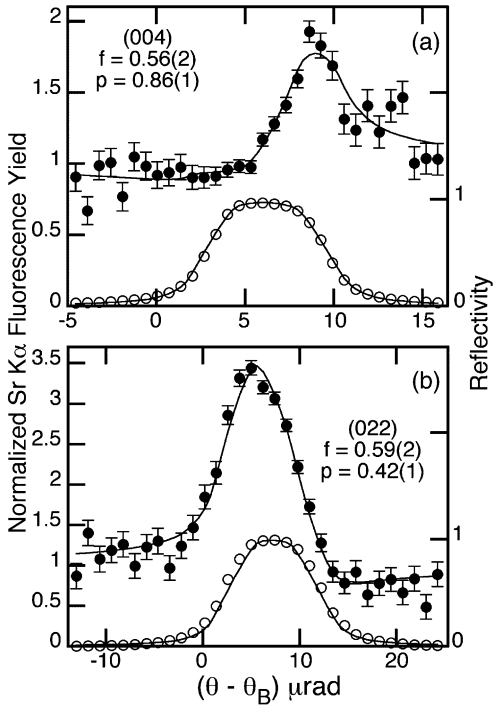

Fig. 2. Reflectivity (open circles) and normalized Sr Kα fluorescence yield (solid circles) experimental data along with corresponding theoretical fits for the (a) Si(0 0 4) and (b) Si(0 2 2) XSW measurements made on the surface annealed at 800 °C.

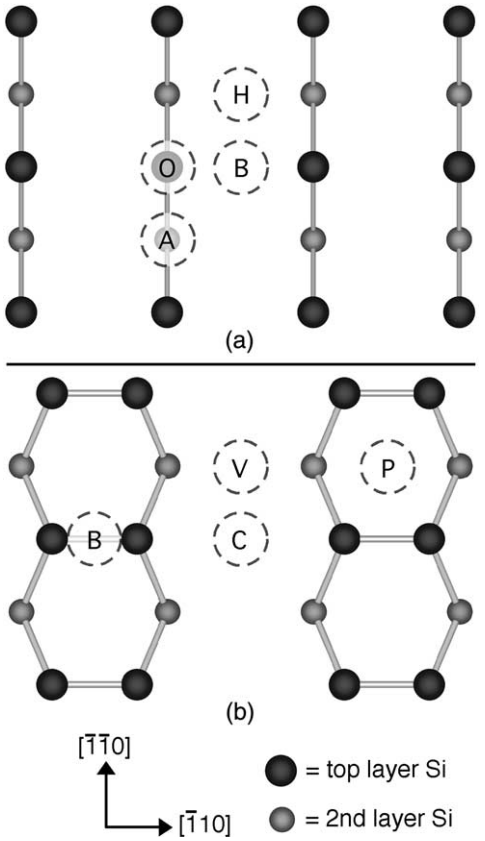

Fig. 3. (a) High-symmetry sites on the undimerized Si(0 0 1) surface: anti-bridge (**A**), on-top (**O**), bridge (**B**), and hollow (**H**). (b) High-symmetry sites on the dimerized surface: bridge (**B**), cave (**C**), valley-bridge (**V**), and pedestal (**P**).

$$P_{111} = \frac{(1 + P_{004})}{4} \tag{5}$$

for one domain and:

$$P_{111} = \frac{(2 + P_{004})}{4} \tag{6}$$

for the other domain. Using Eq. (3), we calculate an expected P_{111} value of 0.59 for Sr atoms located in cave sites at a height corresponding to the experimentally measured $P_{004} = 0.86$. The general agreement between this computed value and the experimentally measured $P_{111} = 0.63$ provides further evidence that the ordered Sr atoms reside at cave or bridge sites.

If we employ D_H values computed using the mean square vibrational amplitude of 0.11 Å reported for Sr in $SrSi_2$ [20], the experimentally measured f_H, and a_H values appropriate for single site ordering in Eq. (1), we obtain respective C values of 0.67, 0.68 and 0.63 based on the Si(0 0 4), Si(0 2 2) and Si(1 1 1) measurements. The close agreement among these values supports our assumption that Sr is ordered onto only one site. If multiple sites were preferentially occupied, the a_H assumed here would differ from the "true" a_H by different amounts for each H, and significant variation would almost certainly be expected among the computed values for C.

These XSW results, combined with our coverage measurements, support three possible models for a 1/6 ML (2×3) phase of Sr/Si(0 0 1). Sr could occupy: (I) 1/3 of the bridge sites on dimerized Si, (II) 1/3 of the cave sites on dimerized Si or (III) 1/6 of the bridge sites on undimerized Si. Since the XSW measurements provide no information about the Si surface atoms, and as mentioned earlier, the sites occupied by Sr in all three of these models represent equivalent positions within the bulk primitive Si unit cell, we must consider additional experimental evidence in order to choose the most plausible of the three models.

If the interpretations of XPS results indicating the presence of surface states due to Si dimers at Sr coverages as high as 1 ML [21] and STM images [12,13] that appeared to show intact Si dimers on the (2×3) Sr/Si(0 0 1) surface are correct, we can immediately rule out model III. The appearance of Si dimers in STM images also provides a reason to exclude model I. If bridge sites were occupied, the Si dimer bonds would either be removed or at least shielded from the STM probe tip by the Sr adatoms. We therefore conclude that model II is the best choice. A top-view [0 0 1] projection of Sr atoms sitting in 1/3 of the cave sites on a dimerized Si(0 0 1) surface is shown in Fig. 4(a) and a side-view [1 1 0] projection of the surface model is shown in Fig. 4(b). The (0 0 4) XSW measured Sr height is 1.17 Å above the bulk-like second layer of Si atoms. While this model is similar to that proposed by Bakhtizin et al. [12,13], the former specifies a vertical position of the Sr atoms and consists of Sr occupying 1/3 rather than 2/3 of the cave sites.

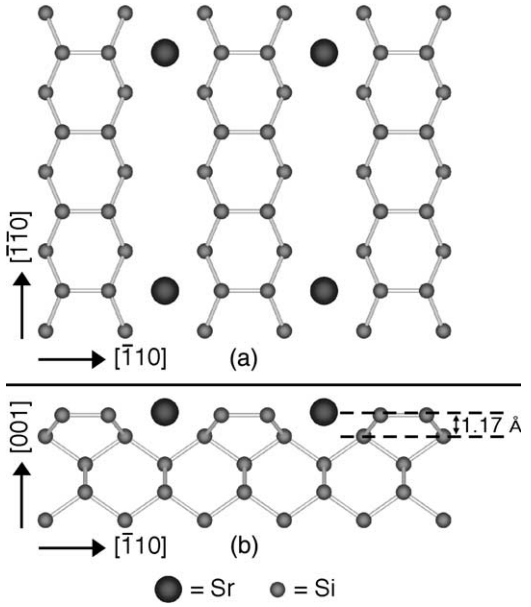

Fig. 4. Model of the 1/6 ML (2×3) surface with Sr occupying 1/3 of the cave sites of the dimerized Si(0 0 1) surface: (a) top-view [0 0 1] and (b) side-view [1 1 0] projections.

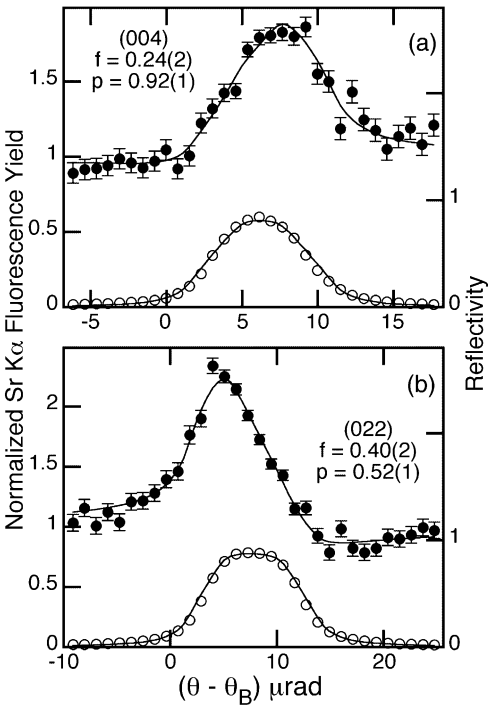

Fig. 5. Reflectivity (open circles) and normalized Sr Kα fluorescence yield (solid circles) experimental data along with corresponding theoretical fits for the (a) Si(0 0 4) and (b) Si(0 2 2) XSW measurements made on the surface annealed at 750 °C.

3.3. XSW analysis of the 750 °C surface

Fig. 5 shows the experimental data and theoretical fits from normal Si(0 0 4) and off-normal Si(0 2 2) XSW measurements of the 750 °C surface, and the model-independent f_H and P_H obtained from these measurements are included in Table 1. Several aspects of this data are inconsistent with the model we just proposed for the 800 °C surface. The P_H values determined for the 750 °C surface are greater than their counterparts from the 800 °C surface and deviate significantly from Eq. (4). Additionally, the f_H values obtained for the 750 °C surface are lower than those measured after the higher anneal temperature and, if used in Eq. (1) assuming a single site for the ordered Sr (i.e. $a_{004} = a_{022} = 1$), yield ordered fractions $C = 0.29$ using f_{004} and $C = 0.46$ using f_{022}. The large discrepancy between these values of the ordered fraction suggests that the a_H used to compute them were incorrect and that consequently, Sr occupies multiple sites on the 750 °C surface.

Density Functional Theory calculations of alkaline earth metal atoms on Si(0 0 1) have indicated that the valley-bridge site is the minimum energy adsorption site for Sr [22] and Ba [23]. STM investigations of the initial stages of Ba deposition on RT Si(0 0 1) [23,24] did in fact show that most of the adatoms were located at valley-bridge sites and that these Ba atoms induced local c(4×2) ordering in the surrounding Si dimers. A STM investigation of Ba deposited onto a Si(0 0 1) substrate held at 900 °C [25] determined that a majority of the Ba atoms were believed to occupy bridge sites forming a (2×3) phase, but a significant fraction was still found in the RT favored valley-bridge site. The 4× streaks that sometimes co-exist with (2×3) and c(2×6) LEED patterns in the 1/6–1/3 ML coverage regime of Ba on Si(0 0 1) [26] are most likely due to the portion Ba atoms at valley-bridge sites inducing c(4×2) ordering in surrounding Si dimers. It is reasonable to propose that the 4× streaks we have observed co-existing with the (2×3) LEED pattern (Fig. 1) of a Sr/

Si(0 0 1) surface annealed at 720 °C are due to Sr located at valley-bridge sites. This proposed model is supported by the presence of small regions of a secondary phase in the STM images of the (2×3) phase of Sr on Si(0 0 1) in Refs. [12,13]. Although it is not discussed in the text, these regions seem to consist of atoms sitting slightly higher than those in the (2×3) phase and are similar in appearance to the features identified as Ba at valley-bridge sites in Ref. [25]. If a portion of the ordered Sr were located at a secondary site, but these secondary adatoms were sufficiently dispersed, the pure (2×3) LEED pattern of the 750 °C surface would still be expected. While short-range ordered Sr atoms would simply contribute to the background of the LEED image, XSW measurements would be sensitive to both their presence and their particular position. In order to incorporate the possibility of both cave and valley-bridge site occupancy into our XSW analysis of the 750 °C surface, we consider the geometrical symmetry relationship:

$$P_{022} = \frac{(1 + P_{004})}{2} \tag{7}$$

(expected if the ordered fraction of Sr were to reside exclusively at the valley-bridge site) in conjunction with Eq. (2) when calculating the expected f_H and P_H. We place the additional constraint that the position of cave site Sr atoms on the 750 °C surface must be at the same height as that determined for the 800 °C surface. For an ordered fraction $C = 0.54$, respective cave and valley-bridge site occupancies of 70% and 30%, and valley-bridge adsorbed Sr atoms located 1.68 Å above the plane of second layer bulk-like Si atoms, we obtain $P_{004} = 0.92$, $f_{004} = 0.24$, $P_{022} = 0.48$ and $f_{022} = 0.40$, in close agreement with the experimental results.

4. Conclusions

We have used LEED and XSW to characterize the atomic scale structure of the Sr/Si(0 0 1)-(2×3) surface phase and present an atomic-scale model consisting of 1/6 ML of Sr atoms in cave sites located 1.17 Å above the bulk-like second layer of Si atoms. When the surface is prepared by RT Sr deposition followed by annealing at 800 °C, the ordered fraction of Sr resides exclusively at the cave site. The (2×3) phase was also formed after annealing at 750 °C, but XSW analysis of this surface is consistent with a significant amount of short-range ordered Sr occupying valley-bridge sites at a height of 1.68 Å above the bulk plane of second layer Si.

Acknowledgements

The authors gratefully acknowledge the BESSRC-CAT staff and O. Auciello of MSD/ANL for assistance with XSW experiments along with L. Funk and P. Baldo of MSD/ANL for providing the RBS calibrated Sr-implanted standard used for coverage determination. We also thank R.A. McKee and F.J. Walker for valuable advice. This work was supported by NSF under contract nos. DMR-9973436, DMR-0076097 and CHE-9810378 and by the DOE-BES under contract no. W-31-109-Eng-38 to ANL and DE-FG02-03ER15457 to NU.

References

[1] A. Mesarwi, W.C. Fan, A. Ignatiev, J. Appl. Phys. 68 (1990) 3609.
[2] W.C. Fan, A. Mesarwi, A. Ignatiev, J. Vac. Sci. Technol. A 8 (1990) 4017.
[3] W.C. Fan, N.J. Wu, A. Ignatiev, Phys. Rev. B 42 (1990) 1254.
[4] H. Maeda, Y. Tanaka, M. Fukutomi, T. Asano, Jpn. J. Appl. Phys. 27 (1988) L209.
[5] M. Lorenz, H. Borner, H. Hochmuth, K. Unger, Physica C 215 (1993) 445.
[6] A.I. Kingon, J.P. Maria, S.K. Streiffer, Nature 406 (2000) 1032.
[7] H. Yuan, R.S. Williams, Chem. Mater. 2 (1990) 695.
[8] K.J. Hubbard, D.G. Schlom, J. Mater. Res. 11 (1996) 2757.
[9] R.A. McKee, F.J. Walker, M.F. Chisholm, Phys. Rev. Lett. 81 (1998) 3014.
[10] J. Ramdani et al., Appl. Surf. Sci. 159–160 (2000) 127.
[11] X. Hu, Z. Yu, J.A. Curless, R. Droopad, K. Eisenbeiser, J.L. Edwards Jr., W.J. Ooms, D. Sarid, Appl. Surf. Sci. 181 (2001) 103.

[12] R.Z. Bakhtizin, J. Kishimoto, T. Hashizume, T. Sakurai, Appl. Surf. Sci. 94–95 (1996) 478.
[13] R.Z. Bakhtizin, J. Kishimoto, T. Hashizume, T. Sakurai, J. Vac. Sci. Technol. B 14 (1996) 1000.
[14] Y. Liang, S. Gan, M. Engelhard, Appl. Phys. Lett. 79 (2001) 3591.
[15] J. Lettieri, J.H. Haeni, D.G. Schlom, J. Vac. Sci. Technol. A 20 (2002) 1332.
[16] A. Ishizaka, Y. Shiraki, J. Electrochem. Soc. 133 (1986) 666.
[17] J. Zegenhagen, Surf. Sci. Rep. 18 (1993) 199.
[18] M.J. Bedzyk, L.W. Cheng, Rev. Miner. Geochem. 49 (2002) 221.
[19] R.A. McKee, F.J. Walker, M.B. Nardelli, W.A. Shelton, G.M. Stocks, Science 300 (2003) 1726.
[20] G.E. Pringle, Acta Cryst. B 28 (1972) 2326.
[21] A. Herrera-Gómez, F.S. Aguirre-Tostado, Y. Sun, P. Pianetta, Z. Yu, D. Marshall, R. Droopad, W.E. Spicer, J. Appl. Phys. 90 (2001) 6070.
[22] R. Droopad et al., J. Cryst. Growth 251 (2003) 638.
[23] X. Yao, X.M. Hu, D. Sarid, Z. Yu, J. Wang, D.S. Marshall, R. Droopad, J.K. Abrokwah, J.A. Hallmark, W.J. Ooms, Phys. Rev. B 59 (1999) 5115.
[24] X. Hu et al., Surf. Sci. 457 (2000) L391.
[25] X. Hu, X. Yao, C.A. Peterson, D. Sarid, Z. Yu, J. Wang, D.S. Marshall, R. Droopad, J.A. Hallmark, W.J. Ooms, Surf. Sci. 445 (2000) 256.
[26] X. Hu, C.A. Peterson, D. Sarid, Z. Yu, J. Wang, D.S. Marshall, R. Droopad, J.A. Hallmark, W.J. Ooms, Surf. Sci. 426 (1999) 69.